

# Electronic and magnetic properties of Lu and LuH<sub>2</sub>

Shunda Zhang,<sup>1,\*</sup> Jiachang Bi,<sup>1,\*</sup> Ruyi Zhang,<sup>1,\*</sup> Peiyi Li,<sup>1</sup> Fugang Qi,<sup>1</sup> Zhiyang Wei,<sup>1</sup> and Yanwei Cao<sup>1,2,†</sup>

<sup>1</sup>*Ningbo Institute of Materials Technology and Engineering, Chinese Academy of Sciences, Ningbo 315201, China*

<sup>2</sup>*Center of Materials Science and Optoelectronics Engineering,*

*University of Chinese Academy of Sciences, Beijing 100049, China*

(Dated: March 21, 2023)

Clarifying the electronic and magnetic properties of lutetium, lutetium dihydride, and lutetium oxide is very helpful to understand the emergent phenomena in lutetium-based compounds (such as room-temperature superconductivity). However, this kind of study is still scarce at present. Here, we report on the electronic and magnetic properties of lutetium metals, lutetium dihydride powders, and lutetium oxide powders. Crystal structures and chemical compositions of these samples were characterized by X-ray diffraction and X-ray photoemission spectroscopy, respectively. Electrical transport measurements show that the resistance of lutetium has a linear behavior depending on temperature, whereas the resistance of lutetium dihydride powders is independent of temperature. More interestingly, paramagnetism-ferromagnetism-spin glass transitions were observed at near 240 and 200 K, respectively, in lutetium metals. Our work uncovered the complex magnetic properties of Lu-based compounds.

arXiv:2303.11063v1 [cond-mat.mtrl-sci] 20 Mar 2023

---

\* These authors contributed equally to this work

† [ywcao@nimte.ac.cn](mailto:ywcao@nimte.ac.cn)

## I. INTRODUCTION

Due to the discovery of room-temperature superconductivity in nitrogen-doped lutetium (Lu) hydrides, the study of Lu-based compounds attracts a great deal of attention very recently [1–5]. Theoretical predication of high-temperature superconductivity in Lu hydrides ( $\sim 273$  K at the pressure 100 GPa in  $\text{LuH}_6$ ) has been reported in the year 2020 [6, 7]. Experimental observation of superconductivity (with the critical temperature  $T_C \sim 15$  K at the pressure 128 GPa) was realized in  $\text{LuH}_3$  in 2021 [8, 9]. Then, the superconductivity critical temperature was increased to 71 K at the pressure 218 GPa in the compound  $\text{Lu}_4\text{H}_{23}$  [2]. However, whether near-ambient superconductivity can exist in Lu-based compounds is still an open question [1–5].

Besides the superconductivity, several other intriguing properties were also reported in Lu-based compounds such as high electrical conductivity and strong spin-orbit coupling in lutetium monoxide LuO [10], phase transformations in the Lu metal and  $\text{LuH}_3$  [11, 12], ultrawide bandgap (5.5-5.9 eV) and luminescence in  $\text{Lu}_2\text{O}_3$  [13, 14]. The element Lu with electron configuration  $4f^{14}5d^16s^2$  is the last one of 14 rare-earth elements. Generally, the valence states of Lu can be  $\text{Lu}^0$ ,  $\text{Lu}^{2+}$ , and  $\text{Lu}^{3+}$  at ambient. Interestingly, superconductivity was observed the in the compounds with  $\text{Lu}^0$  or  $\text{Lu}^{2+}$  or  $\text{Lu}^{3+}$  valence state [1, 8]. Clarifying the electronic and magnetic properties of lutetium-based compounds is very helpful to understand the emergent phenomena. However, this kind of study is still scarce at present [15, 16].

To address the above, we investigated the structural, electronic, and magnetic properties of  $\text{Lu}^0$  metals,  $(\text{Lu}^{2+})\text{H}_2$  powders, and  $(\text{Lu}^{3+}_2)\text{H}_3$  powders with X-ray diffractometer (XRD), X-ray photoemission spectroscopy (XPS), electrical transport, and

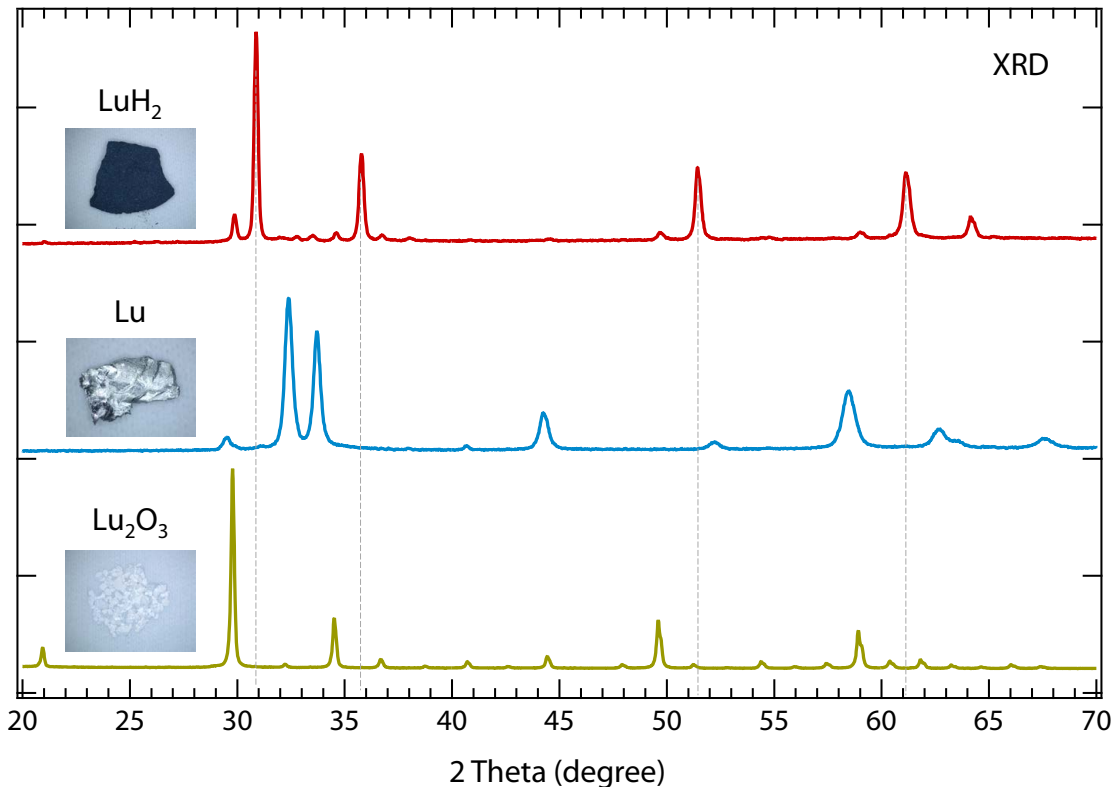


FIG. 1. XRD data of Lu metals,  $\text{LuH}_2$  powders, and  $\text{Lu}_2\text{O}_3$  powders at room temperature. The insets show photographs of three samples. The colours of Lu metals,  $\text{LuH}_2$  powders (compressed), and  $\text{Lu}_2\text{O}_3$  powders are silvery white, dark blue, and white, respectively.

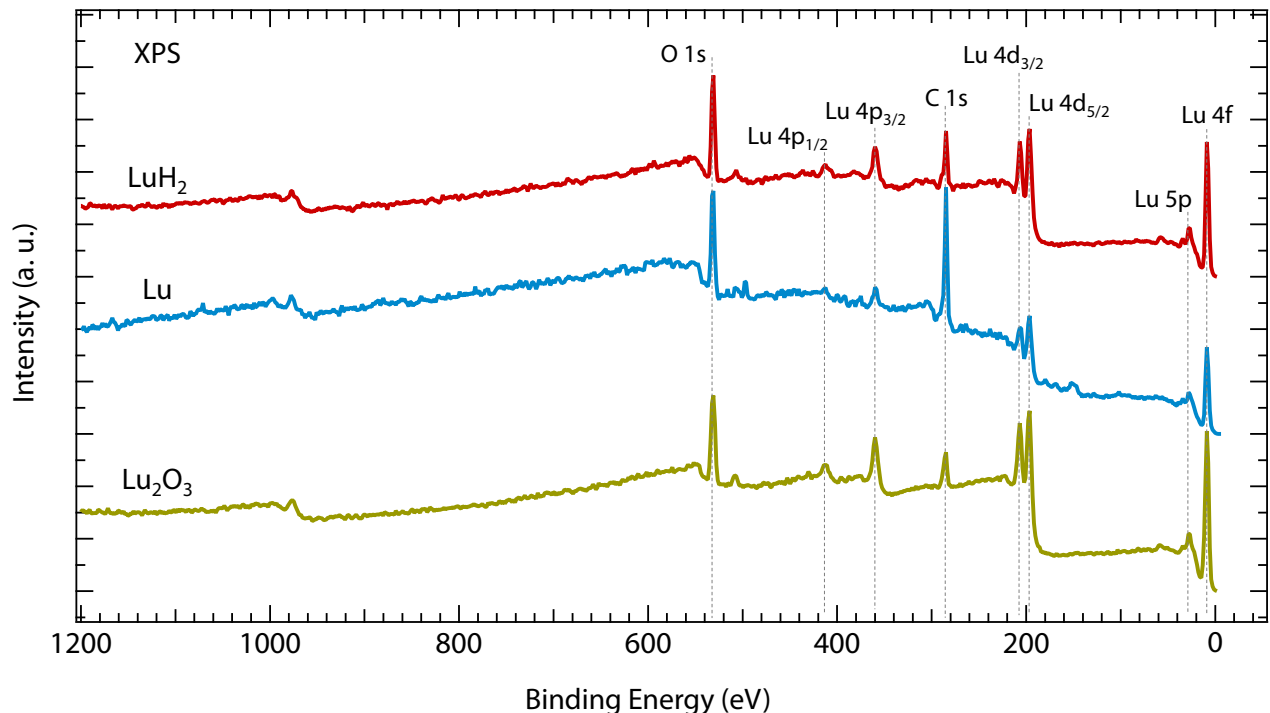


FIG. 2. XPS spectra of Lu metals, LuH<sub>2</sub> powders, and Lu<sub>2</sub>O<sub>3</sub> powders from 0 to 1200 eV at room temperature.

a magnetometer with the superconducting quantum interference device (SQUID). It is revealed that both LuH<sub>2</sub> and Lu show complex magnetic transitions.

## II. EXPERIMENTS

All samples (Lu polycrystalline metals, LuH<sub>2</sub> powders, and Lu<sub>2</sub>O<sub>3</sub> powders, see the insets in Fig.1) studied in this work are commercial. The Lu polycrystalline metals (silvery white) were ordered from Griem Advanced Materials (China), whereas the dark blue LuH<sub>2</sub> powders (misabeled as “Lu”, purity of 99.9%, analogous to the samples reported in ref. 4) and white Lu<sub>2</sub>O<sub>3</sub> powders were purchased from Macklin (China). The  $2\theta - \omega$  scans on three samples were carried out by a powder XRD (Bruker D8 Discover) with the Cu K <sub>$\alpha$</sub>  source. To characterize the chemical compositions of samples, XPS (monochromatic Al K <sub>$\alpha$</sub>  radiation,  $h\nu = 1486.6$  eV, Kratos AXIS Supra) was performed at room temperature. The electrical properties were measured from 300 to 2 K by Physical Property Measurement System (PPMS) in a van der Pauw geometry (DynaCool, Quantum Design). To measure the electrical transport of LuH<sub>2</sub>, it is noted that the LuH<sub>2</sub> powders were compressed into several tablets at room temperature. Temperature-dependent magnetic properties were characterized by a SQUID magnetometer from the temperature 300 to 2 K.

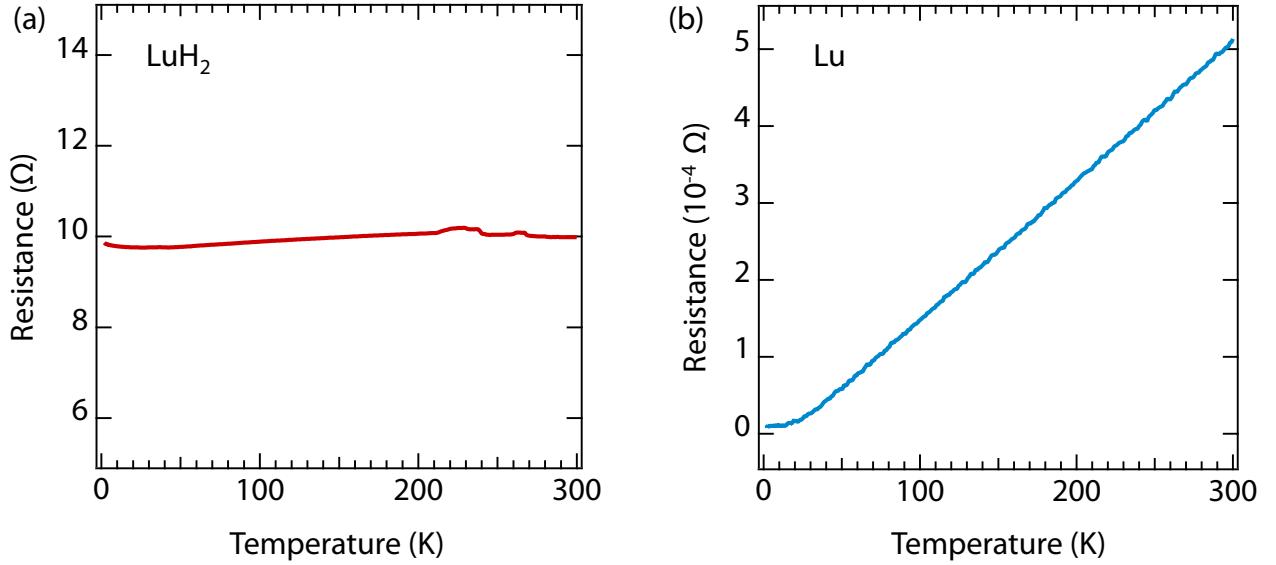


FIG. 3. Temperature-dependent resistances of (a) LuH<sub>2</sub> powders (compressed) and (b) Lu metals from 300 to 2 K.

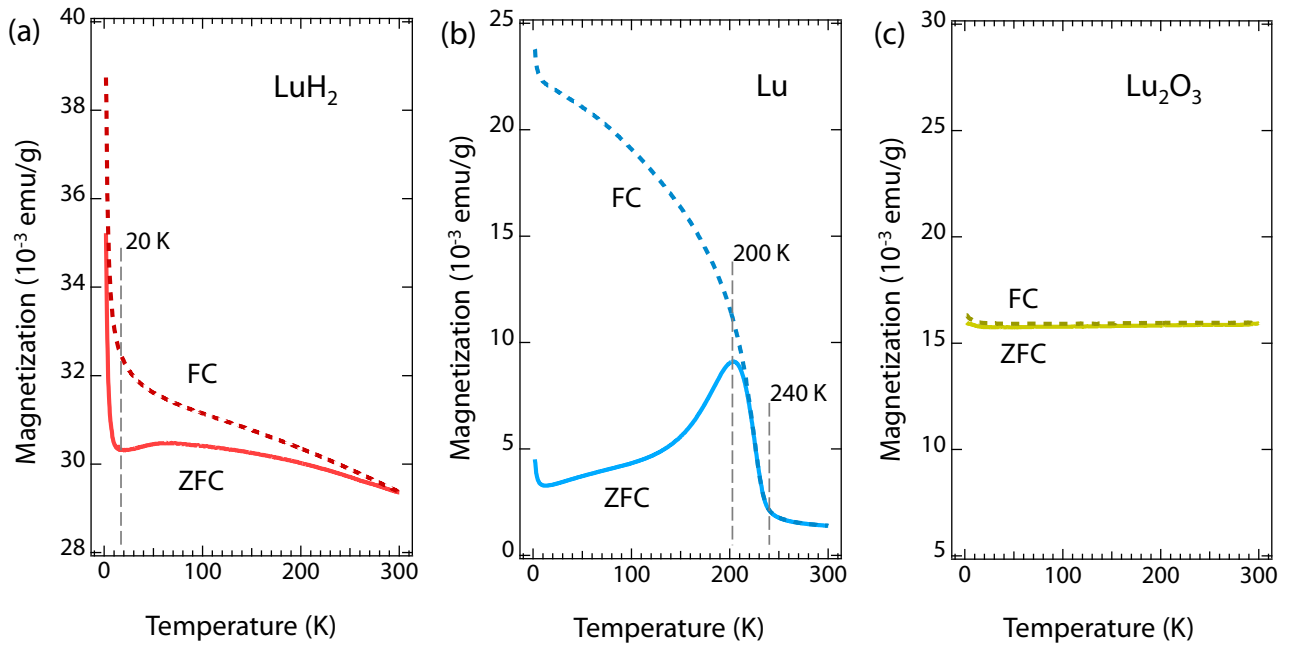


FIG. 4. Temperature-dependent magnetizations (ZFC and FC) of LuH<sub>2</sub> powders (compressed), Lu metals, and Lu<sub>2</sub>O<sub>3</sub> powders from 300 to 2 K. During measurements, the cooling field was set at 1000 Oe.

### III. RESULTS AND DISCUSSION

First, we explored the crystal structures of these three samples. As shown in Fig. 1, the diffraction peaks of these three samples are totally different. The dominative feature of LuH<sub>2</sub> XRD data (see the red curve in Fig. 1) is the four main diffraction peaks in the range 20-70 degrees, which agrees well with the previous report [4]. The crystal structure of LuH<sub>2</sub> is cubic (Fm $\bar{3}$ m

space group) with an estimated lattice parameter  $a \sim 5.03\text{\AA}$ . Also, it is noteworthy that several small peaks can be seen in the XRD curve of LuH<sub>2</sub>. Compared to the XRD lineshapes of Lu and Lu<sub>2</sub>O<sub>3</sub> (see blue and red curves in Fig. 1), it is indicated that the LuH<sub>2</sub> sample has little Lu and Lu<sub>2</sub>O<sub>3</sub> compositions, which is consistent with the previous report [4].

To further investigate the chemical compositions of Lu, LuH<sub>2</sub>, and Lu<sub>2</sub>O<sub>3</sub> samples, we performed XPS at room temperature, which is a surface-sensitive technique to probe the valence states of compounds. As seen in Fig.2, apart from the oxygen (O 1s  $\sim 531$  eV) and carbon (C 1s  $\sim 284.8$  eV) existed on sample surfaces, no distinct impurities is detected, verifying the purity of these samples. Interestingly, a number of peaks can be observed in the XPS spectra, most of which are assigned to Lu core-level states such as Lu 4*f* ( $\sim 9$  eV), 5*p* ( $\sim 28$  eV), 4*d*<sub>5/2</sub> ( $\sim 196$  eV), 4*d*<sub>3/2</sub> ( $\sim 207$  eV), 4*p*<sub>3/2</sub> ( $\sim 360$  eV), and 4*p*<sub>1/2</sub> ( $\sim 411$  eV) states [17]. Here, we emphasize that the surfaces of both Lu and LuH<sub>2</sub> are easily oxidized.

Next, we characterized the electronic properties of Lu and LuH<sub>2</sub> samples by electrical transport from 300 to 2 K. As shown in Fig. 3, both Lu (size  $\sim 3.7 \times 1.9 \times 0.5$  mm<sup>3</sup>) and LuH<sub>2</sub> (size  $\sim 5.1 \times 6.1 \times 0.8$  mm<sup>3</sup>) are highly conducting, the resistances of which are  $\sim 10$   $\Omega$  and  $\sim 10^{-4}$   $\Omega$ , respectively. With decreasing the temperature from 300 to 2 K, the resistance of LuH<sub>2</sub> is almost independent of temperature, whereas the resistance of Lu shows a strong linear behavior down to 20 K, then becomes a constant below 20 K. The resistance of Lu changed from  $5.13 \times 10^{-4}$   $\Omega$  at 300 K to  $0.1 \times 10^{-4}$   $\Omega$  at 20 K. It is noted that the data in Fig. 3 (a) is noisy due to the measured LuH<sub>2</sub> sample in Fig. 3 (a) being a compressed tablet from LuH<sub>2</sub> powders.

At last, to investigate the magnetic properties of Lu, LuH<sub>2</sub>, and Lu<sub>2</sub>O<sub>3</sub>, we measured the zero-field cooling (ZFC) and field cooling (FC) magnetization curves by SQUID. During measurements, the cooling field was set at 1000 Oe. As seen in Fig. 4, Lu, LuH<sub>2</sub>, and Lu<sub>2</sub>O<sub>3</sub> present totally different magnetic properties. For LuH<sub>2</sub>, the magnetization under FC protocol (see the dashed red curve in Fig. 4(a)) increases monotonously with decreasing the temperature to 20 K, whereas the magnetization has a bump ( $\sim 60$  K) for the ZFC protocol (see the solid red curve in Fig. 4(a)). Comparing to LuH<sub>2</sub> in Fig. 4(a), unexpectedly, the behavior of temperature-dependent magnetization of Lu is more complicated. As shown in Fig. 4(b), there is a distinct separation between ZFC and FC curves, which can result from the spin-glass transition [18–20]. With decreasing the temperature from 300 to 2 K, two critical features (at  $\sim 240$  K and  $\sim 200$  K) can be observed. The first one  $\sim 240$  K can be interpreted as the paramagnetic to the ferromagnetic phase transition, whereas the second one  $\sim 200$  K is due to a spinglass transition. In contrast to Lu and LuH<sub>2</sub>, the magnetizations of Lu<sub>2</sub>O<sub>3</sub> are almost independent of temperature, indicating the diamagnetic nature of Lu<sub>2</sub>O<sub>3</sub> [21].

#### IV. CONCLUSION

In this work, we characterized the electronic and magnetic properties of Lu, LuH<sub>2</sub>, and Lu<sub>2</sub>O<sub>3</sub> by XRD, XPS, electrical transport, and SQUID. Both Lu and LuH<sub>2</sub> are metallic, whereas Lu<sub>2</sub>O<sub>3</sub> is insulating. The resistance of Lu has a linear behavior depending on temperature, whereas the the resistance of LuH<sub>2</sub> is almostly independent of temperature. More interestingly, the magnetization of both Lu and LuH<sub>2</sub> show a spinglass feature. Our work uncovered unexpected magnetic properties of Lu-based compounds.

#### V. ACKNOWLEDGMENTS

We thank Xinming Wang, Jie Sun, and Kemin Jiang for helping experimental setup. We acknowledge insightful discussions with Baomin Wang and Shaozhu Xiao. This work was supported by the National Key R&D Program of China (Grant No. 2022YFA1403000), the National Natural Science Foundation of China (Grant Nos. U2032126 and 11874058), the Pioneer

Hundred Talents Program of the Chinese Academy of Sciences, the Zhejiang Provincial Natural Science Foundation of China under Grant No. LXR22E020001, the Beijing National Laboratory for Condensed Matter Physics, the Ningbo Natural Science Foundation (Grant No. 20221JCGY010338), and the Ningbo Science and Technology Bureau (Grant No. 2022Z086).

- 
- [1] N. Dasenbrock-Gammon Snider, E. McBride, R. Pasan, H. Durkee, D. Khalvashi-Sutter, N. Munasinghe, S. Dissanayake, S. E. Lawler, K. V. Salamat, A. Dias, R. P., Evidence of near-ambient superconductivity in a N-doped lutetium hydride, *Nature* **615**, 244 (2023).
- [2] Z. Li, X. He, C. Zhang, K. Lu, B. Bin, J. Zhang, S. Zhang, J. Zhao, L. Shi, and S. Feng, Superconductivity above 70 K experimentally discovered in lutetium polyhydride, arXiv:2303.05117 (2023).
- [3] M. Liu, X. Liu, J. Li, J. Liu, Y. Sun, X.-Q. Chen, and P. Liu, On parent structures of near-ambient nitrogen-doped lutetium hydride superconductor, arXiv:2303.06554 (2023).
- [4] P. Shan, N. Wang, X. Zheng, Q. Qiu, Y. Peng, and J. Cheng, Pressure-induced color change in the lutetium dihydride LuH<sub>2</sub>, *Chinese Phys. Lett.* (2023).
- [5] X. Ming, Y.-J. Zhang, X. Zhu, Q. Li, C. He, Y. Liu, B. Zheng, H. Yang, and H.-H. Wen, Absence of near-ambient superconductivity in LuH<sub>2±x</sub>N<sub>y</sub>, arXiv:2303.08759 (2023).
- [6] H. Song, Z. Zhang, T. Cui, C. J. Pickard, V. Z. Kresin, and D. Duan, High T<sub>c</sub> superconductivity in Heavy Rare Earth hydrides: correlation between the presence of the *f* states on the Fermi surface, nesting and the value of T<sub>c</sub>, arXiv:2010.12225 (2020).
- [7] M. Du, H. Song, Z. Zhang, D. Duan, and T. Cui, Room-Temperature Superconductivity in Yb/Lu Substituted Clathrate Hexahydrides under Moderate Pressure, *Research* **2022**, 9784309 (2022).
- [8] M. Shao, S. Chen, W. Chen, K. Zhang, X. Huang, and T. Cui, Superconducting ScH<sub>3</sub> and LuH<sub>3</sub> at Megabar Pressures, *Inorg. Chem.* **60**, 15330 (2021).
- [9] D. Wang, Y. Ding, and H.-K. Mao, Future Study of Dense Superconducting Hydrides at High Pressure, *Materials* **14**, 7563 (2021).
- [10] K. Kaminaga, D. Oka, T. Hasegawa, and T. Fukumura, New Lutetium Oxide: Electrically Conducting Rock-Salt LuO Epitaxial Thin Film, *ACS omega* **3**, 12501 (2018).
- [11] G. N. Chesnut and Y. K. Vohra, Phase transformation in lutetium metal at 88 GPa, *Phys. Rev. B* **57**, 10221 (1998).
- [12] M. Tkacz and T. Palasyuk, Pressure induced phase transformation of REH<sub>3</sub>, *J. Alloys Compd.* **446**, 593 (2007).
- [13] D. Zhang, W. Lin, Z. Lin, L. Jia, W. Zheng, and F. Huang, Lu<sub>2</sub>O<sub>3</sub>: A promising ultrawide bandgap semiconductor for deep UV photodetector, *Appl. Phys. Lett.* **118**, 211906 (2021).
- [14] S. Matsumoto and A. Ito, Chemical vapor deposition route to transparent thick films of Eu<sup>3+</sup>-doped HfO<sub>2</sub> and Lu<sub>2</sub>O<sub>3</sub> for luminescent phosphors, *Opt. Mater. Express* **10**, 899 (2020).
- [15] R. S. Lee and S. Legvold, Hall Effect of Gadolinium, Lutetium, and Yttrium Single Crystals, *Phys. Rev.* **162**, 431 (1967).
- [16] F. H. Spedding and J. J. Croat, Magnetic properties of high purity yttrium, lanthanum, and lutetium and the effects of impurities on these properties, *J. Chem. Phys.* **59**, 2451 (1973).
- [17] V. V. Kaichev, T. I. Asanova, S. B. Erenburg, T. V. Perevalov, V. A. Shvets, and V. A. Gritsenko, Atomic and Electronic Structures of Lutetium Oxide Lu<sub>2</sub>O<sub>3</sub>, *J. Exp. Theor. Phys.* **116**, 323 (2013).
- [18] J. A. Mydosh, *Spin Glasses: An Experimental Introduction* (Taylor & Francis, London, 1993).
- [19] F. Wang, J. Kim, and Y. Kim, Spin-glass behavior in LuFe<sub>2</sub>O<sub>4+δ</sub>, *Phys. Rev. B* **80**, 024419 (2009).
- [20] W. Huang, X. Zhang, H. Du, R. Yang, Y. Tang, Y. Sun, and Z. Cheng, Intrinsic exchange bias effect in phase-separated La<sub>0.82</sub>Sr<sub>0.18</sub>CoO<sub>3</sub> single crystal, *J. Phys.: Condens. Matter* **20**, 445209 (2008).
- [21] L. Ben Farhata, M. Amamib, E.K. Hlil, and R. Ben Hassen, Synthesis, structure and magnetic properties of the Lu<sub>2</sub>O<sub>3</sub>-CoO mixed system, *Mater. Chem. Phys.* **123**, 737 (2010).